The RoadMapping Code: How to deal with "Real World" Issues in Action-based Dynamical Modelling the Milky Way

W. Trick[1,2], J. Bovy[3,4], and H.-W. Rix[1]

trick@mpia.de

Subject headings: Galaxy: disk — Galaxy: fundamental parameters — Galaxy: kinematics and dynamics — Galaxy: structure

Contents

[1]Max-Planck-Institut für Astronomie, Königstuhl 17, D-69117 Heidelberg, Germany

[2]Correspondence should be addressed to trick@mpia.de.

[3]Institute for Advanced Study, Einstein Drive, Princeton, NJ 08540, USA

[4]Hubble fellow

1. Introduction

[TO DO]

Collection of thoughts for the introduction: *(Text is not yet perfect or concise, but should serve as a starting point to setup a basic structure for the introduction. The text will then have to be shortened, redundant formulations have to be removed, phrasing has to be improved and everything has to be supported with appropriate references.)*

- RoadMapping stands for "Recovery of the Orbit/Action Distribution of Mono-Abundance Populations and Potential INference for our Galaxy".
- **Our modelling method in a nutshell:** We fit simultaneously a model for the Galaxy's gravitational potential and an orbit distribution function (df) to stellar phase-space data. To turn a star's position and velocity into a full orbit, we need the gravitational potential in which the star moves. We assume that we know a family of orbit distribution functions that are close enough to the real distribution of orbits. In this case the stellar orbits calculated within a proposed potential will only follow such a df, if this potential model is close enough to the true potential.
  Or in other words: We need the potential to calculate orbits. At the same time, if we *know* the true orbits, we can deduce the true potential from them. To find the true orbits, we make use of the predictive power of an orbit distribution function.
- **Introducing orbits and actions:** There are different ways to describe stellar orbits. The most obvious is to give the stars position and velocity vector at each point in time, by evaluating the potential forces that act on the star in each time step. Most orbits in realistic galaxy potentials are however not closed, so we would have to integrate the orbit forever. Another, much more convenient way to describe orbits, are so called integrals of motion. These integrals are functions of the star's time-dependent position and velocity, but are themselves constants in time, i.e. conserved quantities. The most obvious integral in static potentials is the energy of the orbit. Symmetries in potentials frequently allow more than one integral: In spherical potentials all three components of the angular momentum are conserved. In many axisymmetric potentials there is, in addition to the energy E and vertical component of the angular momentum L_z, a third non-classical integral of motion I_3, which has however no easy physical meaning. (Binney & Tremaine, Galactic Dynamics)
  Because any function of integrals is an integral of motion itself, it is possible to construct integrals that have both very convenient properties and intuitive physical meanings.

One such a set are the so-called actions. In axisymmetric potentials they are frequently called the radial action J_R, the vertical action J_z and the ϕ-action, which is simply the vertical component of the angular momentum, L_z. The radial action and vertical action quantify the amount of oscillation in radial and vertical direction that the orbit exhibits. Actions are constructed in such a way, that they are not only integrals, but also correspond to the momenta in a set of canonical coordinates. The canonical conjugate positions of the actions are the so-called angles, which have the convenient properties, that they increase strictly linearly in time while the star moves along the orbit. They are periodic in 2π and the frequencies by which they change are functions of the actions. In the action-angle coordinate system, the only thing we need to fully describe an orbit in an axisymmetric potential are therefore just three fixed numbers, the actions.

- **Using actions for distribution functions:** Actions are therefore the natural coordinates of orbits and each point in action space corresponds to one specific orbit in a given potential. It is often used in dynamical modelling, e.g. in the Schwarzschild superposition method (source???), to reconstruct a galaxy by superimposing different orbits and populating them with stars. In this way these kind of methods construct orbit distribution functions for galaxies, which are at the same time distribution functions in action space. Because angles increase linearly in time, when a star moves along its orbit, stars are uniformly distributed in angle space. Therefore a orbit distribution function in terms of actions and a uniform distribution of stars in angle-space can be directly mapped to a distribution of stars in canonical configuration phase-space, measurable stellar positions and velocities. While a stellar distribution in configuration space is six-dimensional, the distribution in action-angle space is effectively three-dimensional, because of the uniformity in angles. (Rewrite, too verbose...)

- **Motivation to use Binney's qDF in the modelling:** Astronomers consider galaxies frequently as a superposition of several components. The stellar component itself is often separated into bulge, halo and several disk sub-populations. Distribution functions in terms of actions have the advantage, that a full distribution function for the whole galaxy can be constructed by a superposition of action-based DFs for each component. [TO DO: This was what Payel Das told me, but I forgot why this is the case and I also didn't find any reference for this. ???] Assuming a DF with a simple form for each galaxy component can give, in superposition, very realistic looking, flexible and successful models for the distribution of stars in galaxies (Bovy & Rix 2013; Sanders & Binney 2015; Piffl et al. 2014) (other references???). Any dynamical modelling approach still depends crucially the assumption one makes about the structure of the galaxy and on the choices for the DFs:

The structure of the MW disk is still under debate. While many still support the thin-thick disk dichotomy in the MW disk (references ???), Bovy et al. (2012b) found indications that the MW disk might actually be a super-position of many stellar subpopluations with a continuous spectrum of scale heights, scale lengths, metallicity and [α/Fe] abundances (dubbed mono-abundance populations (*MAP*s)). Further investigation lead to the findings that *MAP*s in the MW disk have a simple spatial structure that follows an exponential in both radial and vertical direction (Bovy et al. 2012d). The corresponding velocity dispersion profile of the *MAP*s also decreases exponentially with radius and is nearly independent of height above the plane, i.e. quasi-isothermal (Bovy et al. 2012c). The radial decrease in vertical velocity dispersion has, according to Bovy et al. (2012c), a long scale length of $h_{\sigma,z} \sim 7$ kpc for all *MAP*s . Older *MAP*s , which are characterized by lower metallicities and [α/Fe] abundances, have in general shorter density scale lengths, larger scale heights and velocity dispersion (Bovy et al. 2012d). Ting et al. (2013) and Bovy & Rix (2013) finally proposed that these findings could be employed for dynamical modelling techniques using action-based distribution functions. An action-based distribution function, that is flexible enough to describe the spectrum of simple phase-space distributions of different *MAP*s , is the quasi-isothermal distribution function (qDF) by Binney & McMillan (2011), as demonstrated by Ting et al. (2013).

- **Some caveats of DF assumptions as compared to others:** Sanders & Binney (2015) and ??? develop extended distribution functions (EDFs), that extend action-based DFs to also describe the distribution of the star's metallicities. While a full chemo-dynamical modelling, including metallicity as well as α- and other chemical abundances, is ultimately the right way to go, the form of the EDFs still depends on a lot of additional assumptions. By looking at fig. 6 in Bovy & Rix (2013) (other references???) we doubt that a final version of an EDF will have a simple form in action-metallicity space. Motivated by the findings by Bovy et al. 2012, we therefore resign to the simpler approach outlined in Bovy & Rix (2013) and here, were metallicity and α-abundances are implicitly taken into account by describing each MAP separately by one qDF. This procedure could have two caveats:
  First, the binning of the stars according to their abundances could lead to pollution of one MAP, by either choosing the bin sizes too large, or too small compared to the stars' inherent abundance errors.
  Second, while Ting et al. (2013) makes us confident that the qDF is indeed a good functional form to describe each MAP, it could very well be, that the stars' true distribution is close to but not exactly of the family of assumed qDFs.
  Some comments by HWR regarding Sanders & Binneys take on our mod-

elling, should be also included: [TO DO]

- Overall, there is no doubt that making a simultaneous model for the "chemo-orbital-potential" distribution has some advantages over the "orbital-potential" distribution at a given abundance. The main advantage for pursueing MAP modelling at least as a first/intermediate step is: a) it separates out complexity (i.e. it's much easier to "see" what goes right or wrong), b) it provides true cross-checking redundancy w.r.t. to the potential estimates [TO DO: I don't understand the latter]
- "First, choosing bin sizes always requires a compromise between losing the information contained in the position of each datum within its bin and increasing Poisson noise by making the bins small." –¿ That is true for any binning. But with the realistic samples sizes, bins within which the abundances vary "little" have a sensible number of stars (for SEGUE)
- It is true that the MAP approach does not exploit that the abundance space distribution is "smooth"; however, the data show that there is no "simple and large-scale" pattern that lends itself to a simple functional form.
- " Third, we require errors in the ([Fe/H], [alpha/Fe]) space that are much smaller than the bin sizes, otherwise we are neglecting the possibility of contamination on each bin by neighbouring bins." –¿ I don't think the argument is valid; it wouldn't make sense to make the bins SMALLER than the errors, because then you would reduce the samples size and increase the shot-noise, WITHOUT making the approximation to the model DF better. You could make the bin size larger (therefore the error smaller than the bin-size), but would pay the prize of a poorer approximation. So, I actually would think that making the bin size of order of the abundance error is a sensible choice, if that leaves you with "enough" objects in the bin.
- " Additionally, a continuous parametrization allows for a rigorous treatment of the error distributions in ([Fe/H], [alpha/Fe]) and how these errors correlate with the kinematic errors. Hence we believe that it is best to work with an EDF provided we are confident that we have a sufficiently flexible and well-tailored functional form." –¿I would agree with that statement but a) it's not easy to get a simple form for that, see sigma_z(FeH,aFe) Figures in B12; and the redundance argument from above applies...

- **Why should we care about actions in realistic galaxies?** In reality galaxies have rarely perfectly static and axisymmetric potentials, which drastically reduces the number of conserved quantites along orbits. In static non-axisymmetric potentials

there can still be two integrals of motion, angular momentum however is no longer conserved. The Milky Way's disk might have an overall axisymmetric appearance, but is perturbed by spiral arms. The strongest deviation from axisymmetry in the Galaxy is the bar, which also causes the Galactic potential to vary slowly in time. The stirrs up the stars of the disk and the potential and causes radial migration of the orbits (Reference???), orbits change and with them the actions. One could wonder if, under such non-axisymmetric, non-static potential conditions, the assumption and treatment of globally conserved actions in the Milky Way is still a sensible approach. First of all, actions are the natural way to treat orbits and they can be locally defined, even if they might not be globally conserved. As long as we care about orbits, we should care about actions. An orbit carries information about the star's past, about where the star was born and which tidal processes might have carried it away from its inital orbit. Together with the chemistry of the stars, which determined by their place of birth, their current orbits are valuable diagnostics for the evolution and structure of the Milky Way. Secondly, gravitational processes do only in the most extreme cases completely change the actions. In a slowly changing potential, where orbits adapt adiabatically to those changes, actions are conserved (Binney & Tremaine, Galactic Dynamics). And even during bar-induced radial migration at least the vertical actions are conserved and will continue to carry some amount of information about the stars' inital orbit distribution.

[TO DO] (Maybe cite Potzen 2015, who showed that analysing aspherical systems in spherical actions can still be a powerful tool, when used with care...)

- **Why should we care about an axisymmetric "best fit" model for the Milky Way disk?** One of the key assumptions of our modelling technique is the assumed axisymmetry of the Milky Way's gravitational potential, especially its disk. As we discussed already in the previous paragraph, this assumption is indeed only an approximation to the real disk, which has a much richer structure and more complicated potential, with spiral arms and ring-like structures (like the Monocerros ring), with a warp and a flare in the outer disk (references????). Also the Milky Way's halo has substructure, a multitude of streams (references???) and shell-like overdensities (reference???). The ultimate goal will be to find and identify substructures observationally and describe theoretically the structure and evolution of potential perturbations. Our method and efforts to extract information about the axisymmetric Milky Way potential from disk stars aims to create a reliable and well-constraint basis for these endevours: The best possible axisymmetric approximation to the Milky Way's potential could serve as a realistic equilibrium model from which a description of non-axisymmetric tidal perturbations can be theoretically established by perturbation theory. It will

also help a great deal to identify sub-structures, e.g. to find and orbitally connect tidal streams, which in return will then give better constraints on the deviations from axisymmetry. Many modelling and techniques, both purely gravitational, but also chemo-dynamical, can greatly profit from a good axisymmetric model for the galaxy: While we are still far away from knowing the MW's potential all over the place, an axisymmetric model will be the best reference to turn phase-space coordiantes into whole orbits. And orbits are the diagnostics that carry information from everywhere in the galaxy into the solar neighbourhood, where we can hope to exploit them. (Some overlap with section before. How to better structure these two sections and assign the arguments more clearly to "axisymmetric disk" or "actions"?)

- **Previous results with this modelling technique:** Bovy & Rix (2013) ... [TO DO]
  - disk scale length $R_d = 2.15 \pm 0.14$ kpc (Bovy & Rix 2013)
  - disk is maximal (Bovy & Rix 2013)
  - slope of dark matter halo $\alpha < 1.53$ (Bovy & Rix 2013)
- **What do we already know about the axisymmetric MW disk (from other references)?** [TO DO]
  - rotation curve is well-known (reference???)
- **What is there left to learn about the axisymmetric MW disk?** (as Jo asked at the Santa Barbara conference... [TO DO]
  - separation of different MW component is still unclear: individual density profiles, contributions to total pot
  - thin/thick disk vs. continuum of exponential disks
  - dark matter at smaller radii
  - slope & shape of dark matter halo (current state of knowledge?)
- **Other modelling approaches:**
  - Piffl et al. (2014) used a slightly different DF-based modelling approach to constrain the MW's vertical density profile near the sun. They fitted a superposition of "quasi-isothermal" DFs for thick and thin disk, and a DF for the halo to ˜200,000 giant stars from the RAVE survey (RAdial Velocity Experiment, Steinmetz et al. (2006)). They didn't use any chemical information of the stars. To account for different populations within the thin disk, they weighted the corresponding DF's with an assumed star-formation rate instead. To circumvent the

use of RAVE's non-trivial spatial selection function, they separated stars into spatial bins in (R, z) and fitted the velocity distribution predicted by their DF and potential model at the mean (R, z) of each bin to the observed velocities only. They're result for their radial profile of the vertical force within $|z| = 1.1$ kpc and $R > 6.6$ kpc agrees well with the previous results from our method by Bovy & Rix (2013). By not using chemical information and hiding the spatial distribution of stars by binning to circumvent a complicated selection function, Pifffl et al. (2014) is however rejecting a lot of valuable information in the data set. ([TO DO: Look at other useful references in this paper: Bienayme et al. 2014, Zhang et al. 2013, Binney et al. 2014a, Binney 2012b, McMillan & Binney 2013])

- **Motivating this method characterization in anticipation of GAIA:** [TO DO]
- **Ideas how to structure this introduction:**
  - Part I: Basic task is fitting potential and DF at the same time. This is a great, useful and successful way to constrain the galactic gravitational potential. Was already done in Bovy & Rix (2013).
  - Part II: While Bovy & Rix (2013) were successful in their application, they made many approximations / assumptions / idealisations, which were not tested for their valicity and might actually not hold up well. We want to investigate this. We cannot test everythong, but we show some plausible and illustrative examples (often using a spherical isochrone potential for convenience). (Also mention what Sanders & Binney (2015) say about this modelling approach.)

2. Dynamical Modelling

2.1. Model

2.1.1. Actions

[TO DO]

2.1.2. Potential models

[TO DO] Mention different ways to calculate actions in different potentials.

2.1.3. Distribution function

Motivated by the findings of Bovy et al. 2012??? and Ting et al. (2013) about the simple phase-space structure of *MAP*s (see §1), and following Bovy & Rix (2013) and their successful application, we also assume that each *MAP* follows a single qDF of the form given by Binney & McMillan (2011). This qDF is a function of the actions $\boldsymbol{J} = (J_R, J_z, L_z)$ and has the form

$$\mathrm{qDF}(\boldsymbol{J} \mid p_{\mathrm{DF}}) = f_{\sigma_R}(J_R, L_z \mid p_{\mathrm{DF}}) \times f_{\sigma_z}(J_z, L_z \mid p_{\mathrm{DF}}) \quad (1)$$

$$\text{with } f_{\sigma_R}(J_R, L_z \mid p_{\mathrm{DF}}) = n \times \frac{\Omega}{\pi\sigma_R^2(R_g)\kappa}\left[1 + \tanh\left(L_z/L_0\right)\right] \exp\left(-\frac{\kappa J_R}{\sigma_R^2(R_g)}\right) \quad (2)$$

$$f_{\sigma_z}(J_z, L_z \mid p_{\mathrm{DF}}) = \frac{\nu}{2\pi\sigma_z^2(R_g)} \exp\left(-\frac{\nu J_z}{\sigma_z^2(R_g)}\right) \quad (3)$$

$$(4)$$

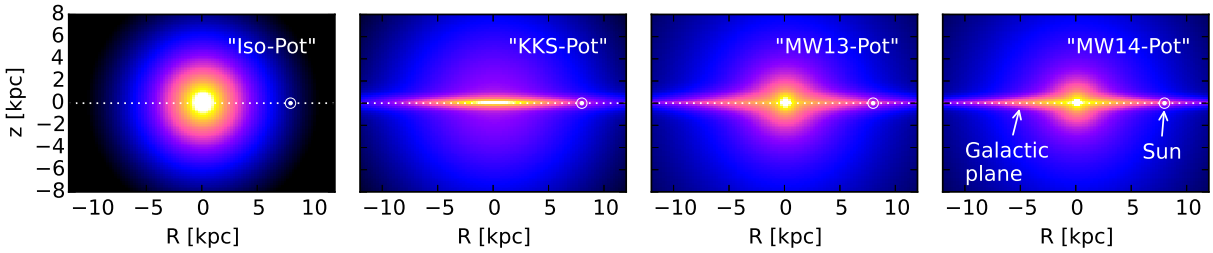

Fig. 1.— Density distribution of the four reference galaxy potentials in table 1, for illustration purposes. These potentials are used throughout this work for mock data creation and potential recovery. [TO DO: Halo sichtbarer machen, evtl. mit isodensity contours]

Table 1. Gravitational potentials of the reference galaxies used troughout this work and the respective ways to calculate actions in these potentials. All four potentials are axisymmetric. The potential parameters are fixed for the mock data creation. In the subsequent analyses we aim to recover these potential parameters again. All reference potentials assume the sun to be located at $(R_\odot, z_\odot) = (8\ \mathrm{kpc}, 0)$.

name	potential type	potential parameters p_Φ		action calculation	reference for potential type
"Iso-Pot"	isochrone potential	circular velocity at the sun	$v_{\mathrm{circ}} = 230\ \mathrm{km\ s^{-1}}$	***analytical and exact*** J_r, J_ϑ, L_z;	Binney & Tremaine (2008)
		isochrone scale length	$b = 0.9$ kpc	use $J_r \to J_R, J_\vartheta \to J_z$	
				in eq. (???)	
"KKS-Pot"	2-component	circular velocity at the sun	$v_{\mathrm{circ}} = 230\ \mathrm{km\ s^{-1}}$	***exact*** J_R, J_z, L_z	Batsleer & Dejonghe (1994)
	Kuzmin-Kutuzov-	focal distance of coordinate system[a]	$\Delta = 0.3$	using "Stäckel Fudge"	
	Stäckel potential	axis ratio of the coordinate surfaces[a] ...		(Binney 2012)	
		...of the disk component	$\left(\frac{a}{c}\right)_{\mathrm{Disk}} = 20$	[in analysis: additional grid	
		...of the halo component	$\left(\frac{a}{c}\right)_{\mathrm{Halo}} = 1.07$	interpolation (Bovy 2015)]	
		relative contribution of the disk mass to the total mass	$k = 0.28$		
"MW13-Pot"	MW-like potential with	circular velocity at the sun	$v_{\mathrm{circ}} = 230\ \mathrm{km\ s^{-1}}$	***approximate*** J_R, J_z, L_z	Bovy & Rix (2013)
	Hernquist bulge,	stellar disk scale length	$R_d = 3$ kpc	using "Stäckel Fudge"	
	2 exponential disks	stellar disk scale height	$z_h = 0.4$ kpc	(Binney 2012)	
	(stars + gas),	relative halo contribution to $v^2_{\mathrm{circ}}(R_\odot)$	$f_h = 0.5$	[in analysis: additional grid	
	spherical power-law halo	"flatness" of rotation curve	$\frac{\mathrm{d}\ln(v_{\mathrm{circ}}(R_\odot))}{\mathrm{d}\ln(R)} = 0$	interpolation (Bovy 2015)]	
"MW14-Pot"	MW-like potential with cutoff power-law bulge, Miyamoto-Nagai stellar disk, NFW halo	-	-	***approximate*** J_R, J_z, L_z (see "MW13-Pot")	Bovy (2015)

[a]The coordinate system of each of the two Stäckel-potential components is $\frac{R^2}{\tau_{i,p}+\alpha_p} + \frac{z^2}{\tau_{i,p}+\gamma_p} = 1$ with $p \in \{\mathrm{Disk}, /\mathrm{Halo}\}$ and $\tau_{i,p} \in \{\lambda_p, \nu_p\}$. Both components have the same focal distance $\Delta = \sqrt{\gamma_p - \alpha_p}$, to make sure that the superposition of the two components itself is still a Stäckel potential. The axis ratio of the coordinate surfaces $\left(\frac{a}{c}\right)_p := \sqrt{\frac{\alpha_p}{\gamma_p}}$ describes the flattness of the corresponding Stäckel component.

Here $R_g \equiv R_g(L_z)$ and $\Omega \equiv \Omega(L_z)$ are the (guidig-center) radius and the circular frequency of the circular orbit with angular momentum L_z in a given potential. $\kappa \equiv \kappa(L_z)$ and $\nu \equiv \nu(L_z)$ are the radial/epicycle (κ) and vertical (ν) frequencies with which the star would oscillate around the circular orbit in R- and z-direction when slightly perturbed (Binney & Tremaine 2008). The term $[1 + \tanh(L_z/L_0)]$ suppresses counter-rotation for orbits in the disk with $L \gg L_0$ which we set to a random small value ($L_0 = 10 \times R_\odot/8 \times v_{\rm circ}(R_\odot)/220$).
For this qDF to be able to incorporate the findings by Bovy et al. 2012??? about the phase-space structure of *MAP*s summarized in §1, we set the functions n, σ_R and σ_z, which indirectly set the stellar number density and radial and vertical velocity dispersion profiles,

$$n(R_g) \propto \exp\left(-\frac{R_g}{h_R}\right) \tag{5}$$

$$\sigma_R(R_g) = \sigma_{R,0} \times \exp\left(-\frac{R_g - R_\odot}{h_{\sigma_R}}\right) \tag{6}$$

$$\sigma_z(R_g) = \sigma_{z,0} \times \exp\left(-\frac{R_g - R_\odot}{h_{\sigma_z}}\right). \tag{7}$$

The qDF for each *MAP* has therefore a set of five free parameters $p_{\rm DF}$: the density scale length of the tracers h_R, the radial and vertical velocity dispersion at the solar position $R_\odot$, $\sigma_R, 0$ and $\sigma_z, 0$, and the scale lengths h_{σ_R} and h_{σ_z}, that describe the radial decrease of the velocity dispersion. The *MAP*s we use for illustration through out this work are summarized in table ???.

[TO DO] [To Do here: Also mention how the density is calculated.]

2.1.4. Selection function: observed volume and completeness

[TO DO]

Table 2. Reference distribution function parameters for the qDF in eq. (1)-(7). These qDFs describe the phase-space distribution of stellar *MAP*s for which mock data is created and analysed throughout this work for testing purposes. The parameters of the "cooler" ("hotter") *MAP*s were chosen such, that the they have the same σ_R/σ_z ratio as the "hot" ("cool") *MAP* . Hotter populations have shorter tracer scale lengths (Bovy et al. 2012d) and the velocity dispersion scale lengths were fixed according to Bovy et al. (2012c).

name of *MAP*	qDF parameters $p_{\rm DF}$				
	h_R [kpc]	σ_R [km s^{-1}]	σ_z [km s^{-1}]	h_{σ_R} [kpc]	h_{σ_z} [kpc]
"hot"	2	55	66	8	7
"cool"	3.5	42	32	8	7
"cooler"	2 +50%	55-50%	66-50%	8	7
"hotter"	3.5-50%	42+50%	32+50%	8	7

3. Results

3.1. What if our assumptions on the (in-)completeness of the data set are incorrect?

The selection function of a survey is described by a spatial survey volume and a completeness function, which determines the fraction of stars observed at a given location within the Galaxy with a given brightness, metallicity etc (see §[TO DO CHECK]). The completeness function depends on the characteristics and mode of the survey, can be very complex and is therefore sometimes not perfectly known. We investigate how much an imperfect knowledge of the selection function can affect the recovery of the potential. We model this by creating mock data with varying incompleteness, while assuming constant completeness in the analysis. The mock data comes from a sphere of $r_{\max} = 3$ kpc around the sun and an incompleteness function that drops linearly with distance r from the sun (fig. 2):

$$\text{completeness}(r) = 1 - \epsilon_r \cdot \frac{r}{r_{\max}} \tag{8}$$

$$\tag{9}$$

This could be understood as a model for the important effect of stars being less likely to be observed the further away they are. We demonstrate that the potential recovery with *RoadMapping* is very robust against somewhat wrong assumptions about the (in-)completeness of the data (see fig. 3). A lot of information about the potential comes from the rotation curve measurements in the plane, which is not affected by applying an incompleteness function.
In Appendix ??? we also show that the robustness is somewhat less striking but still given for small misjudgements of the incompleteness in vertical direction, parallel to the disk plane (fig. **??** and 10). This could model the effect of wrong corrections for dust obscurement in the plane. We also investigate in Appendix ??? if indeed most of the information is stored in the rotation curve. For this we use the same mock data sets as in fig. 3 and 10, but this time we're not including the tangential velocities in the modelling, rather marginalizing the likelihood over v_T. In this case the potential is much less tightly constrained, even for 20,00 stars. For only small deviations of true and assumed completeness ($\lesssim 10\%$) we can however still incorporate the true potential in our fitting result (see fig. **??**).

Stuff that needs to be further examined:

[TO DO] Maybe instead of decreasing completeness with height above the plane, a completeness that INcreases with height above the plan, to model e.g. obscuration due to dust.

[TO DO] Make similar test as isoSphFlexIncompR, but with KKS potential, to test, if this robustness is a special case for the isochrone potential.

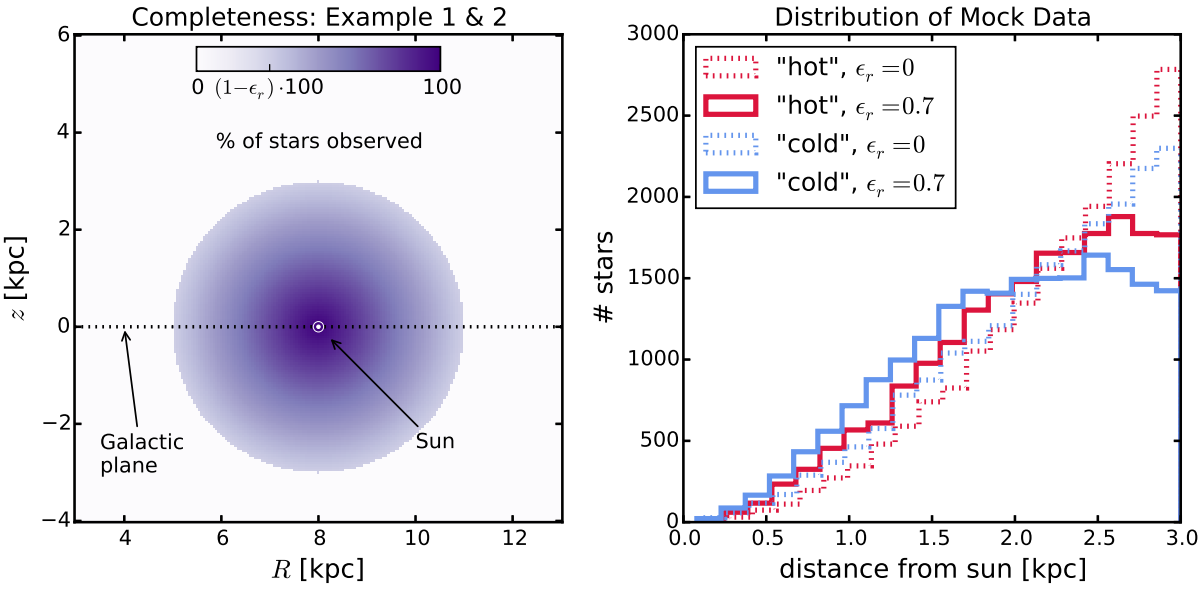

Fig. 2.— [TO DO: Rewrite Caption] Selection function and mock data distribution for investigating radial (Example 1 & 2, left) and vertical (Example 3 & 4, right) incompleteness of the data. The survey volume is a sphere around the sun with $r_{\rm max} = 3$ kpc. In Example 1 & 2 (Example 3 & 4) the percentage of observed stars is decreasing linearly with radius from the sun (height above the Galactic plane), as demonstrated in the first row of panels. How fast this detection rate drops is quantized by the factor ϵ_r (ϵ_z) in eq. (8) (eq. (**??**)). Different mock data sets have different ϵ_r (ϵ_z). Histograms for four data sets, each with 20,000 and drawn from two *MAP*s ("hot" in red and "cool" in blue, see table 2) and with two different ϵ_r (ϵ_z), 0 and 0.7, are shown in the lower two panels for illustration purposes.[TO DO: Re-do, if new analyses are in violin plot.]

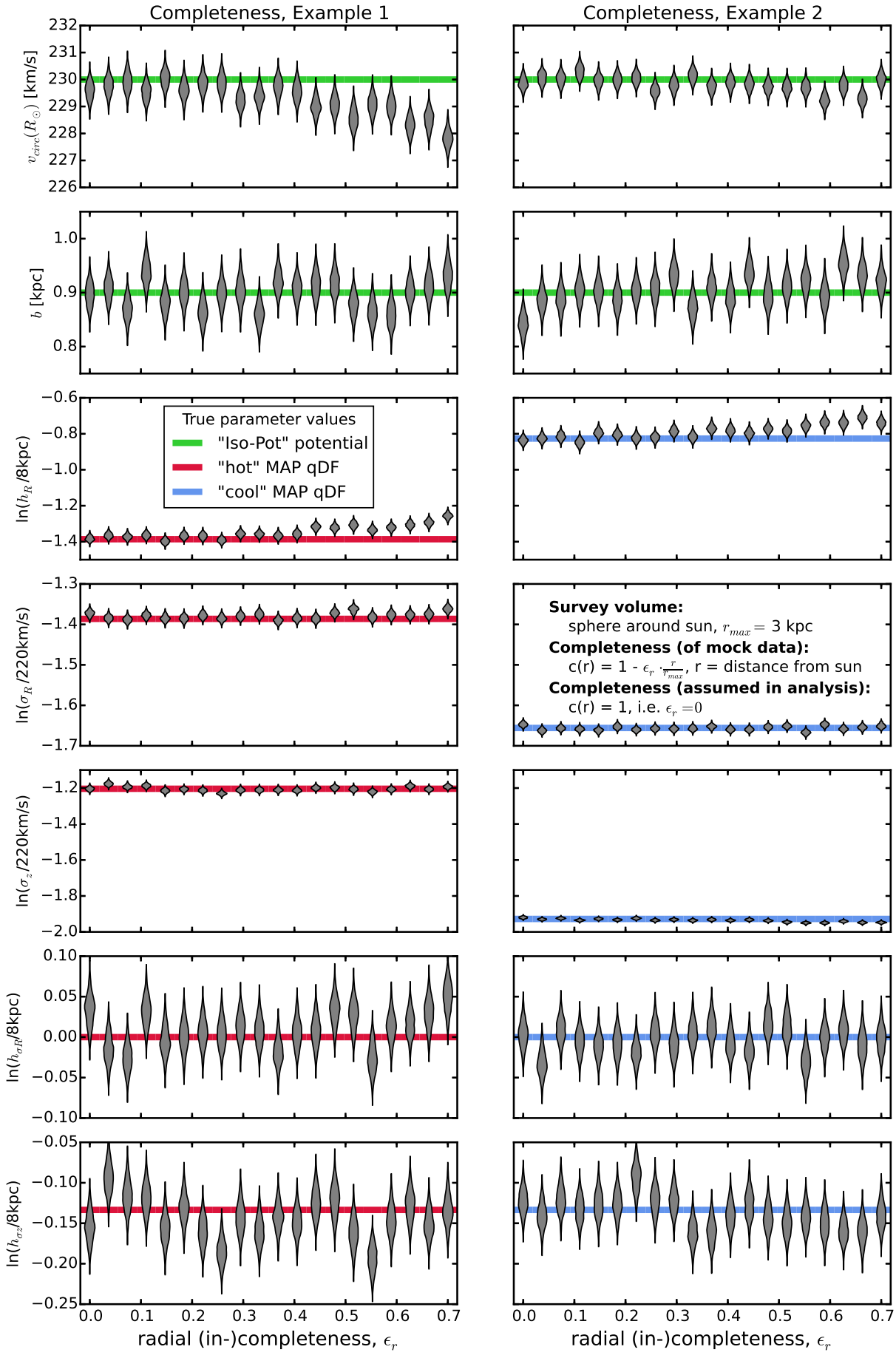

Fig. 3.— Caption [TO DO] (This was done using the current qDF to set the fitting range.

3.2. What if our assumed distribution function differs from the stars' DF?

Our modelling approach is rooted in the assumption that each *MAP* follows a qDF. It could very well be that the true distribution of the stars within one *MAP* , defined by a bin in the [α/Fe]-vs.-[Fe/H]-plane [TO DO: Write consistently.] does indeed slightly differ from our assumed for of the DF. As outlined in §1 this could manifest itself in two ways: Either the qDF is not the correct functional form, or the qDF *is* the proper DF for the *MAP* , but due to too large bin sizes the *MAP*s are polluted by stars from neighbouring *MAP*s .
We try to investigate both this issues with the following test: We draw two mock data sets, each from a different qDF, and mix the stars in different fractions together. We then analyse this mixture by assuming all stars sill came from a single qDF. The results are shown in fig. 5 and 6.
In example 1 and 2 (fig. 5) we consider two very different *MAP*s , a hotter and a cooler one, that are mixed together in different fractions, i.e. the true distribution of stars is a linear combination of two very different qDFs. This test could be understood as a model where the true velocity DF has wider wings or is steeper than the qDF, which generates an approximately Gaussian velocity distribution and the sum of two Gaussians is itself not a Gaussian (see fig. 4). We investigate how this deviation from a single qDF affects the potential recovery. We find that for a *MAP* that follows approximately a hot population (polluted by up to $\sim 30\%$ of cooler stars), the potential can still be very well recovered. The analysis of cooler *MAP*s are much more affected by pollution due to hotter stars.
In example 3 and 4 (fig. 6) it is investigated how different the qDF parameters of two *MAP*s are allowed to be to be still able to constrain the true potential. This test could be seen as a model scenario for decreasing bin sizes in the metallicity-α plane when sorting stars in different *MAP*s assuming that there is a smooth variation of qDF within the metallicity-α plane. We find that, in the case of 20,000 stars in each *MAP* , bin differences of 20% in the qDF parameters of two neighbouring *MAP*s can still give quite good constraints on the potential parameters. We compare this with the relative difference in the qDF parameters in the bins in fig. 6 of Bovy & Rix (2013), which have sizes of $[Fe/H] = 0.1$ dex and $\Delta[\alpha/Fe] = 0.05$ dex. It seems that these bin sizes are large enough to make sure that $\sigma_{R,0}$ and $\sigma_{z,0}$ of neighbouring *MAP*s do not differ more than 20%. As fig. 5 and 6 suggests especially the tracer scale length h_R needs to be recovered to get the potential right. For this parameter however the bin sizes in fig. 6 of Bovy & Rix (2013) might not yet be small enough to ensure no more than 20% of difference in neighbouring h_R, especially in the low-α ($[\alpha/Fe] \lesssim 0.2$), intermediate-metallicity ($[Fe/H] \sim -0.5$) *MAP*s .
In case there are less than 20,000 stars in each *MAP* the constraints are less tight and due to Poisson noise one could also allow larger differences in neighbouring *MAP*s while still getting reliable results.

[TO DO: think, if this might better be two different sections. ???? one for MixDiff about neighbouring MAPS and one for MixCont for difference in DF. ????]

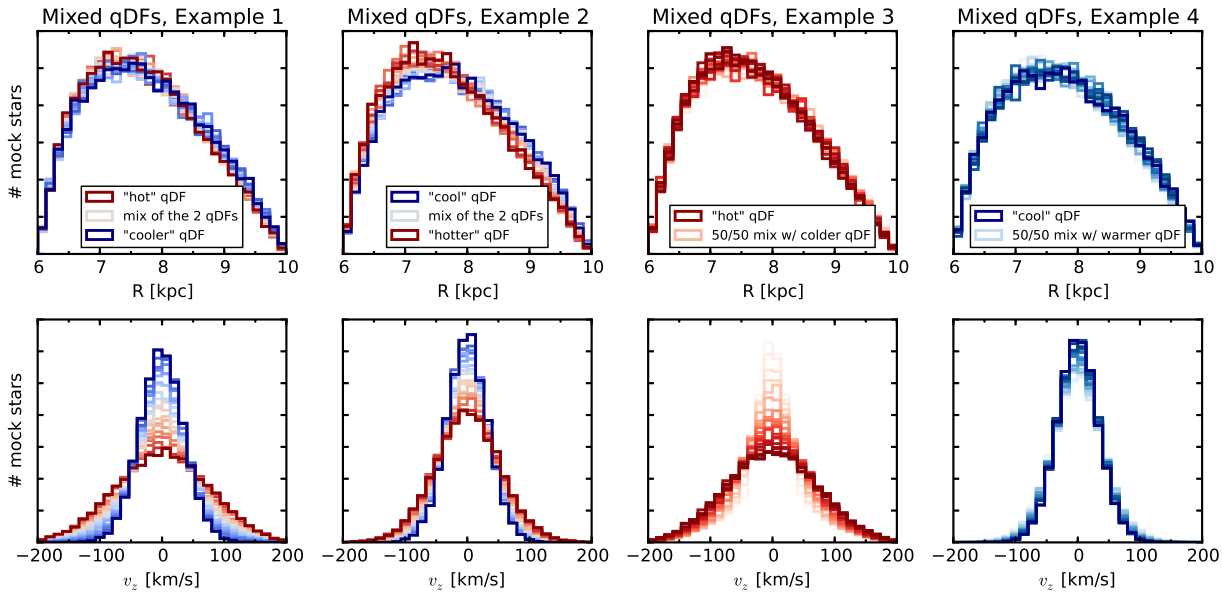

Fig. 4.— Distribution of mock data in two coordinates (R and v_z), created by mixing stars drawn from two different qDFs. This demonstrates how mixing two qDFs can be used as a test case for changing the shape of the DF to not follow a pure qDF anymore, e.g. by adding wings or slightly changing the radial density profile. The distribution in R is also strongly shaped by the selection function, which is, in this case, a sphere around the sun with $r_{\rm max} = 2$ kpc. In total there are always 20,000 stars in each data set and all of them were created in the same potential, the isochrone potential "Iso-Pot" from table 1. The dark red and dark blue histograms show data sets drawn from a single qDF only: the "hot" and "cooler" *MAP*s (Example 1, first column), the "cool" and "hotter" *MAP*s (Example 2, second column), the "hot" (Example 3, third column) and the "cool" *MAP*s (Example 4, fourth column) from table 2. *Example 1 & 2:* The other histograms show data drawn from a superposition of the two reference qDFs. The color coding represents the different mixing rates (reddish: more hot stars, bluish: more cool stars, white: half/half) and is the same as in figure 5, where the corresponding modelling results for each data set are depicted in the same color. *Example 3 & 4:* In this test suite the mixing rate of the two *MAP*s is fixed to 50%/50%. In Example 3 (Example 4) in the third (fourth) column the "hot" ("cool") *MAP* is shown in dark red (dark blue) and mixed with a qDF whose parameters describe a colder (warmer) population. The 'hotness' of these second *MAP* is varied and approaches the "hot" ("cool") *MAP* 's qDF parameters as the histograms get redder (bluer). The color coding is the same as in fig. 6.

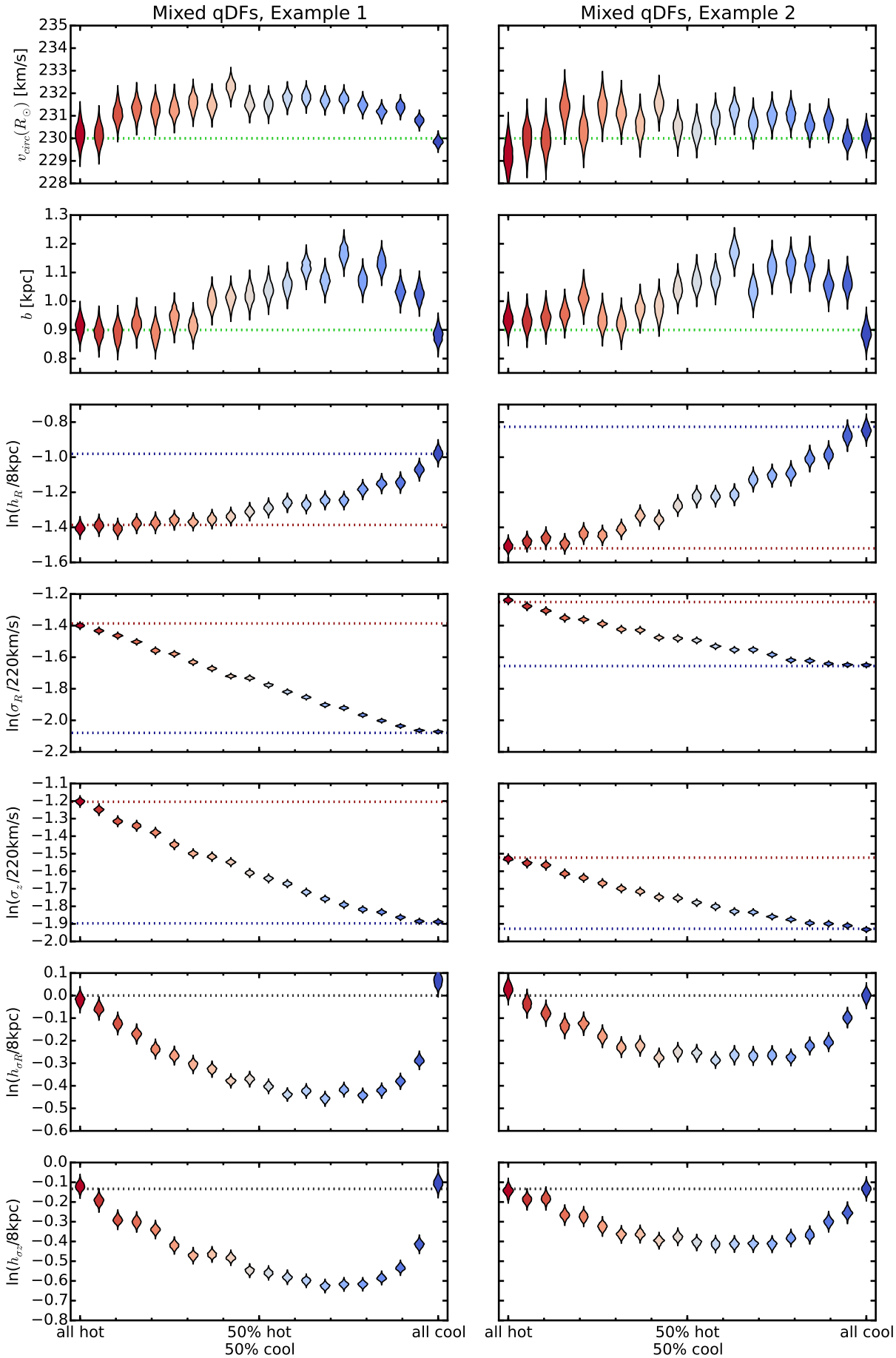

Fig. 5.— (Caption on next page.)

Fig. 5.— (Continued.) The dependence of the parameter recovery on degree of pollution and 'hotness' of the stellar population. To model the pollution of a hot stellar population by stars coming from a cool population and vice versa, we mix varying amounts of stars from two very different populations, as indicated on the x-axis. The composite mock data set is then fit with one single qDF. The violines represent the marginalized likelihoods found from the MCMC analysis. The mock data sets are shown in fig. 4, in the same colors as the violins here. All mock data sets come from the same potential ("Iso-Pot") and selection function (sphere with $r_{\rm max} = 2$ kpc). The true potential parameters are indicated by green dotted lines. Example 1 (Example 2) in the left (right) panels mixes the "hot" ("cool") *MAP* with the "cooler" ("hotter") *MAP* in table 2. True parameters of the hotter (colder) of the two populations are shown as red (blue) dotted lines. We find, that a hot population is much less affected by pollution with stars from a cooler population than vice versa. [TO DO: This was done using the current qDF to set the fitting range. Nvelocity=24 and Nsigma=5 is high enough (though not perfect). Maybe redo with fiducial qDF to be consistent with MixDiff test. ???]

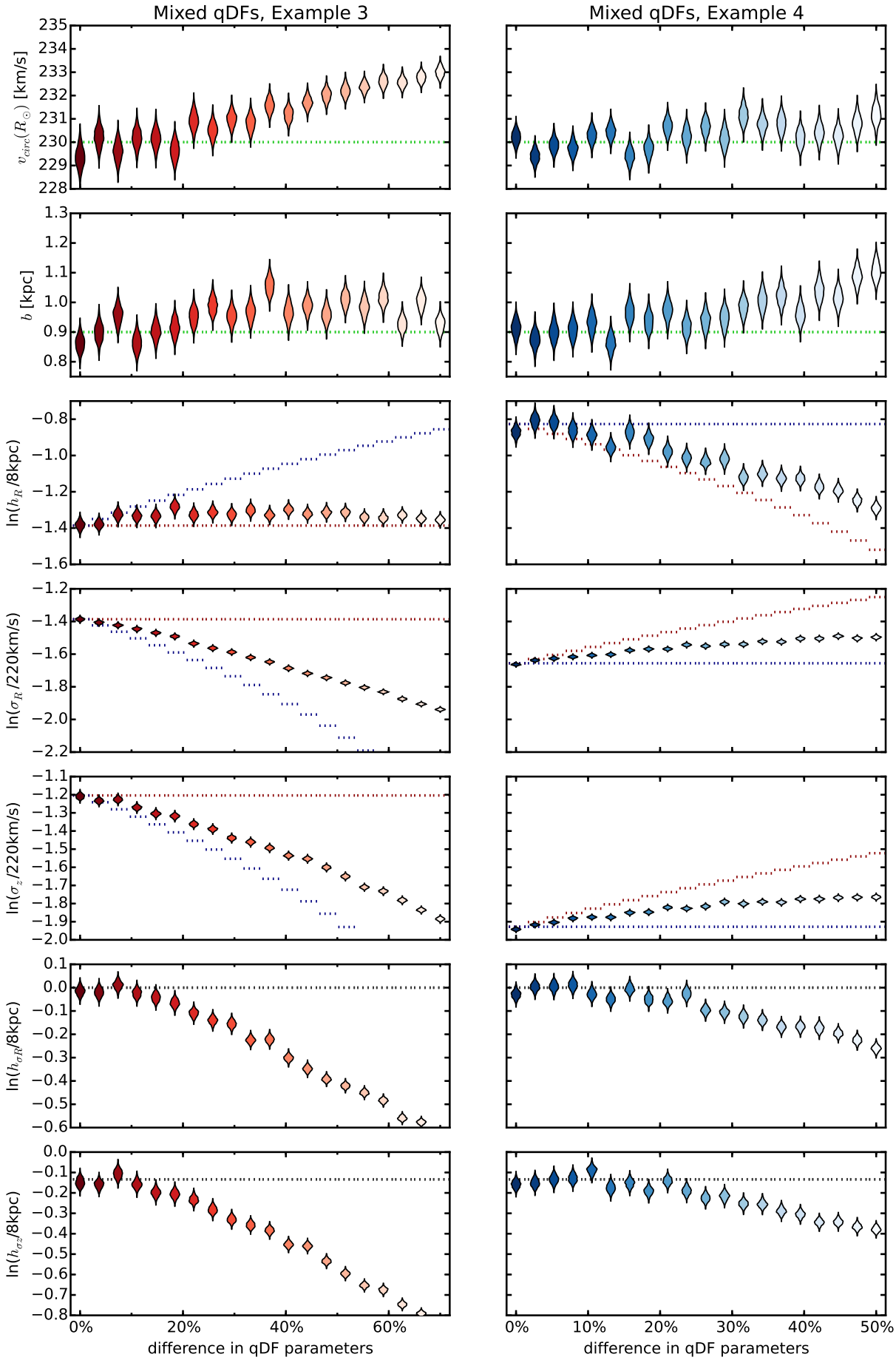

Fig. 6.— (Caption on next page.)

Fig. 6.— (Continued.) The dependence of the parameter recovery on the difference in qDF parameters of the 50%/50% mixture of two stellar populations and their 'hotness'. Each mock data set in Example 3 (Example 4) consists of 20,000 stars, half of them drawn from the "hot" ("cool") qDF in table 2, and the other half drawn from a colder (warmer) population that has X% smaller (larger) σ_R and σ_z and X% larger (smaller) h_R. The difference X in these qDF parameters is indicated on the x-axis, and the true parameters of the two qDFs are indicated by the dotted red and blue lines. Each composite mock data set is fitted by a single qDF and the marginalized MCMC likelihoods for the best fit parameters are shown as violines in the third (fourth) column of panels. The mock data was created within the same potential ("Iso-Pot") and selection function (sphere with $r_{\rm max} = 2$ kpc). The true potential parameters are indicated by green dotted lines. The data sets are shown in figure 4, where the histograms have the same colors as the corresponding best fit violines here. By mixing *MAP*s with varying difference in their qDF parameters, we model the effect of bin size in the [Fe/H]-[α/Fe] plane when sorting stars into different *MAP*s : The smaller the bin size, the smaller the difference in qDF parameters of stars in the same bin. We find that the bin sizes should be chosen such that the difference in qDF parameters between neighbouring *MAP*s is less than 20%. [TO DO: Maybe different/same x-axis???] [TO DO: This was done using the current qDF to set the fitting range. Nvelocity=24 and Nsigma=5 is not high enough for the largest differences, i.e. grid search and MCMC converge to different values. Redo with fiducial qDF.] [TO DO: Add in plot a label, that it is a 50%/50% mix of a hot and a cold population.??])

3.3. What if our assumed potential model differs from the real potential?

Collection of possible tests and plots [TO DO]

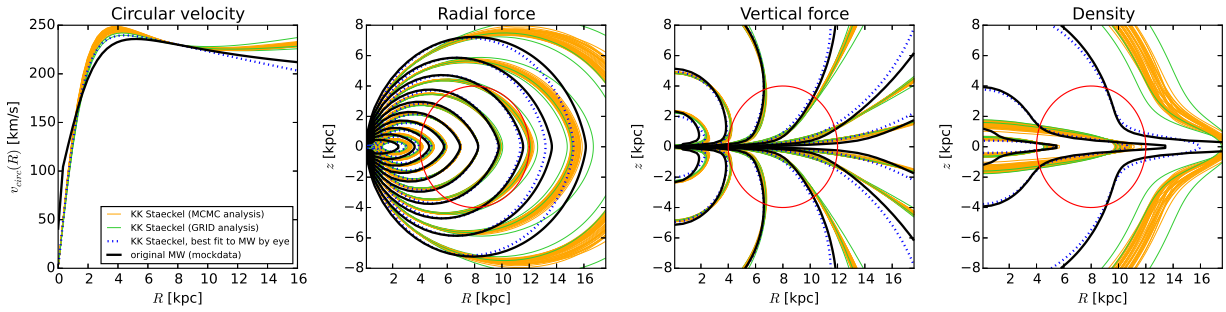

Fig. 7.— [TO DO]

A. Appendix

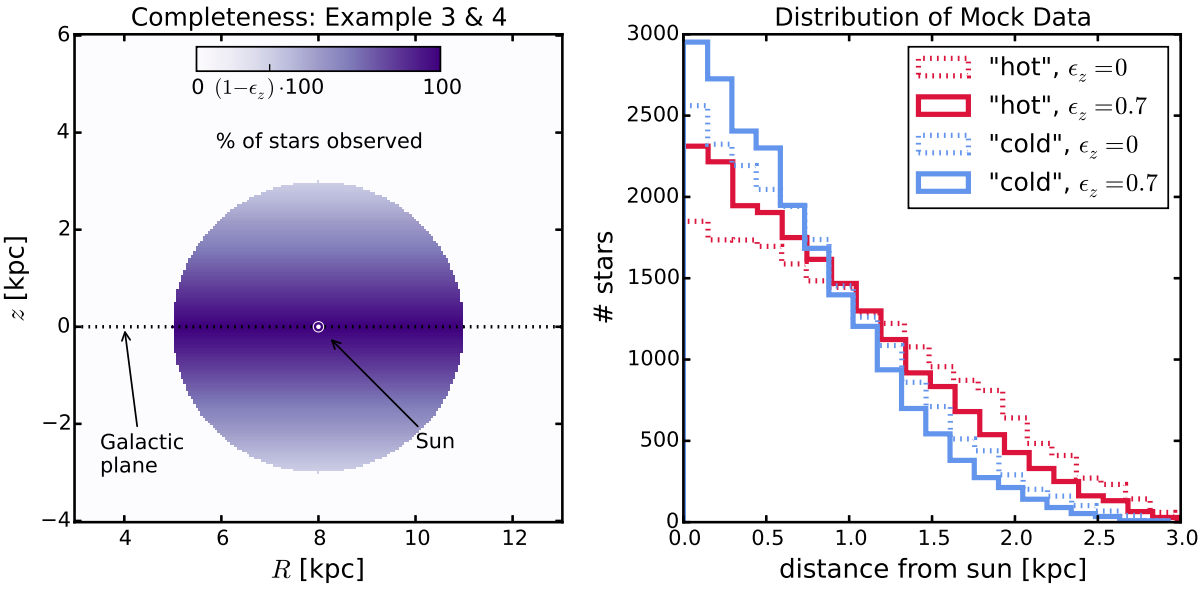

Fig. 8.— [TO DO: Rewrite Caption] Selection function and mock data distribution for investigating radial (Example 1 & 2, left) and vertical (Example 3 & 4, right) incompleteness of the data. The survey volume is a sphere around the sun with $r_{\rm max} = 3$ kpc. In Example 1 & 2 (Example 3 & 4) the percentage of observed stars is decreasing linearly with radius from the sun (height above the Galactic plane), as demonstrated in the first row of panels. How fast this detection rate drops is quantized by the factor ϵ_r (ϵ_z) in eq. (8) (eq. (**??**)). Different mock data sets have different ϵ_r (ϵ_z). Histograms for four data sets, each with 20,000 and drawn from two *MAP*s ("hot" in red and "cool" in blue, see table 2) and with two different ϵ_r (ϵ_z), 0 and 0.7, are shown in the lower two panels for illustration purposes.[TO DO: Re-do, if new analyses are in violin plot.]

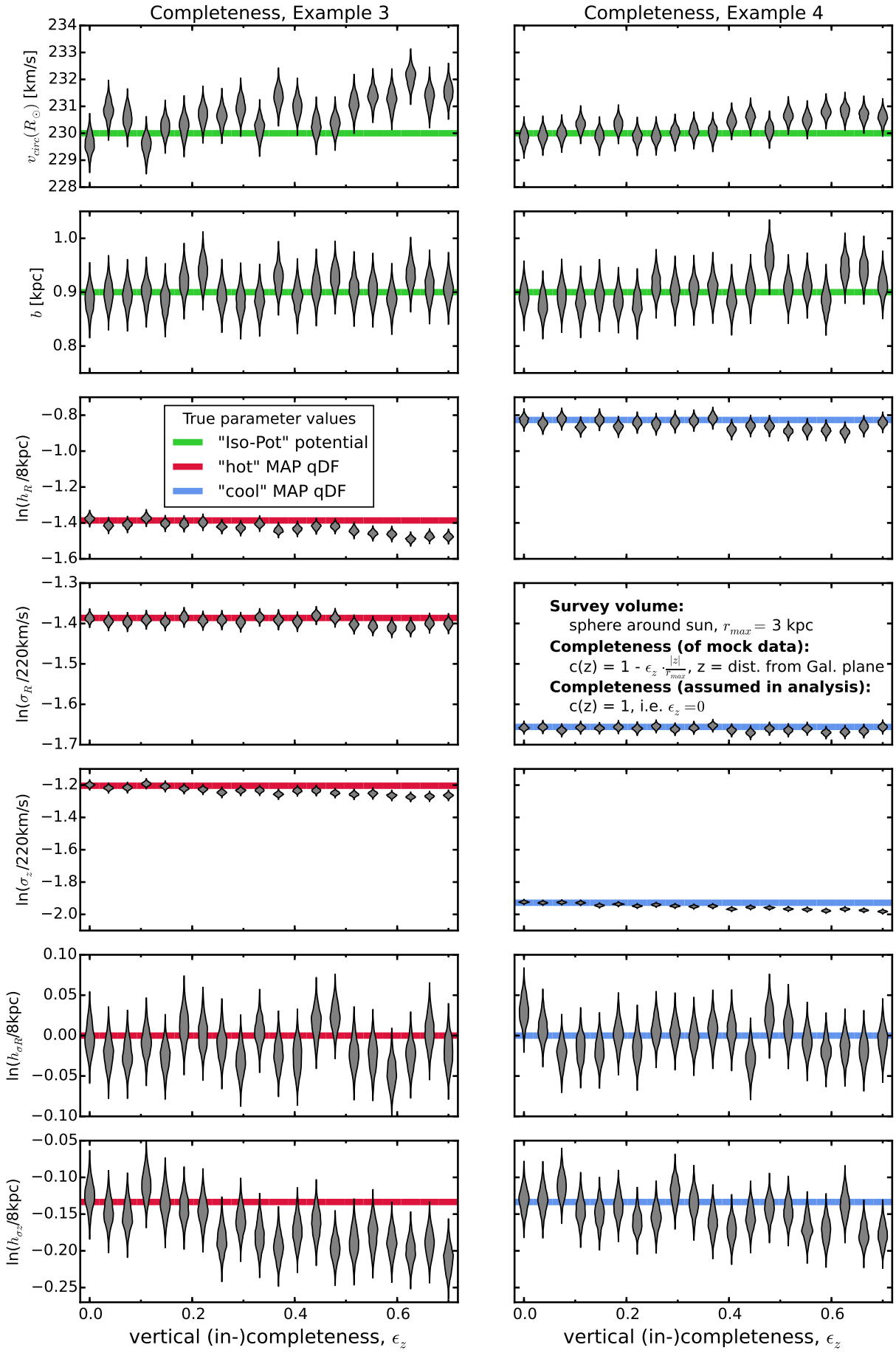

Fig. 9.— Caption [TO DO] (This was done using the current qDF to set the fitting range.

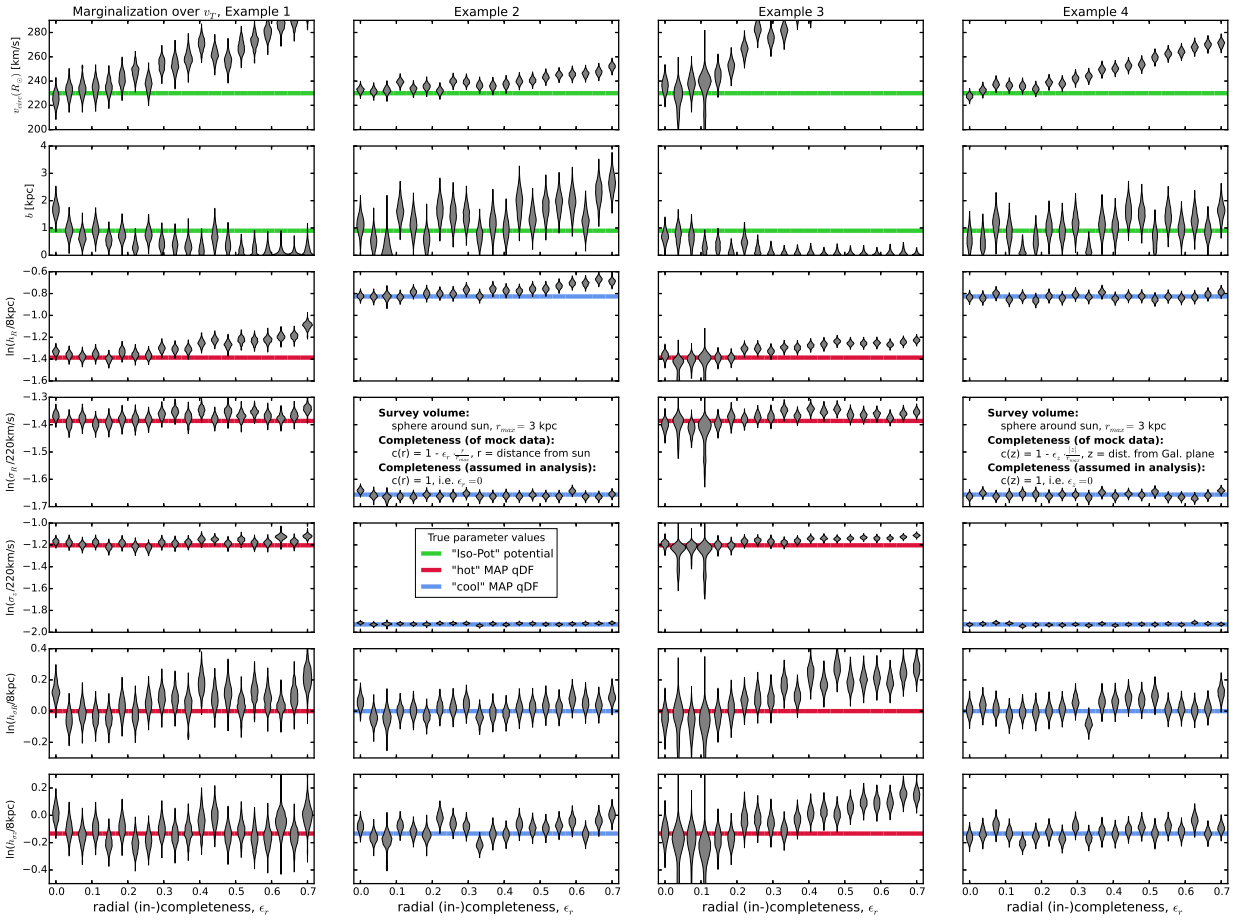

Fig. 10.— Caption [TO DO] ([TO DO: Redo all analyses for which MCMC did not converge to expected peak, and for which b ¡0 was not excluded. ???])

2. Questions that haven't been covered so far:

- What limits the overall code speed?
- What happens, when the errors are not uniform?
- What if errors in distance matter for selection?
- Deviations from axisymmetry: Take numerical simulations.

[TO DO: Check if all references are actually used in paper. ???]

REFERENCES

[TO DO]

Binney, J. J., & McMillan, P. 2011, MNRAS, 413, 1889

Binney, J. J. 2012, MNRAS, 426, 1324

Bovy, J., Rix, H.-W., & Hogg, D. W. 2012b, ApJ, 751, 131

Bovy, J., Rix, H.-W., Hogg, D. W. et al., 2012c, ApJ, 755,115

Bovy, J., Rix, H.-W., Liu, C. et al., 2012d, ApJ, 753, 148

Bovy, J., & Rix, H.-W. 2003, ApJ, 779, 115

Piffl, T., Binney, J., & McMillan, P. J. et al., 2014, MNRAS, 455, 3133

Steinmetz, M. et al., 2006, AJ, 132, 1645

Ting, Y.-S., Rix, H.-W., Bovy, J., & van de Ven, G. 2013, MNRAS, 434, 652

Binney, J., & Tremaine, S. 2008, [TO DO: Galactic Dynamics???]

[TO DO] Sanders & Binney (2015) Extended distribution functions for our Galaxy

[TO DO] Bovy (2015) Galpy paper